THE JOURNAL OF BIOLOGICAL CHEMISTRY
Vol. 273, No. 41, Issue of October 9, pp. 27017–27025, 1998

Printed in U.S.A.

Structural Requirements for *in Vivo* Myosin I Function in *Aspergillus nidulans**

(Received for publication, June 1, 1998, and in revised form, July 30, 1998)

Nir Osherov‡, Roxanne A. Yamashita‡, Yun-Shin Chung, and Gregory S. May§

From the Department of Cell Biology, Baylor College of Medicine, Houston, Texas 77030

We have investigated the minimal requirements of the tail region for myosin I function *in vivo* using the filamentous fungus *Aspergillus nidulans*. The CL3 strain (McGoldrick, C. A., Gruver, C., and May, G. S. (1995) *J. Cell Biol.* 128, 577–587) was transformed with a variety of *myoA* constructs containing mutations in the IQ, TH-1-like, SH3, and proline-rich domains by frameshift or in-frame deletions of the tail domains. The resulting strains contained wild type *myoA* driven by the *alcA* promoter and a mutant *myoA* driven by its endogenous promoter. This strategy allowed for selective expression of the wild type and/or mutant form of MYOA by the choice of growth medium. Proper septation and hyphal branching were found to be dependent on the interaction of the IQ motifs with calmodulin, as well as, the presence of its proline-rich domain. Additionally, a single proline-rich motif was sufficient for nearly wild type MYOA function. Most surprisingly, the SH3 domain was not essential for MYOA function. These studies expand our previous knowledge of the function of MYOA to include roles in hyphal morphogenesis, septal wall formation, and cell polarity, laying the groundwork for more detailed investigations on the function of the various tail domains in MYOA.

Class I myosins appear to be involved in a variety of cellular processes, including cell motility, contractile vacuole function, receptor-mediated endocytosis, protein secretion, maintenance of cytoskeletal organization, and intracellular organelle movement (1, 2). In addition to the highly conserved myosin motor domain, class I myosins possess variable tail regions. In general, the tail of class I myosins consist of the IQ light chain-binding domain, and the tail homology (TH)[1] 1, 2, and 3 domains. The TH-1 domain is rich in basic amino acids, binds to acidic phospholipids, and has an ATP insensitive actin-binding sight. The TH-2 domain is rich in amino acids glycine, proline, and alanine or glycine, proline, and glutamine. The TH-3 domain is an SH3 domain (*Src* homology 3) (3). Class I myosins have been identified in many lower eukaryotes including *Dictyostelium discoideum* (4), *Saccharomyces cerevisiae* (5–7), *Acanthamoeba castellani* (8), and *Aspergillus nidulans* (9). Although class I myosins have been studied in a variety of systems, the elucidation of their function has been complicated by the presence of multiple class I myosins with apparently overlapping function, such that loss of any single myosin I and in some cases deletion of multiple myosins I is not lethal.

The discovery of *myoA* as an essential class I myosin in *A. nidulans* (9) allows us to address many aspects of MYOA function, including regulation by phosphorylation, protein interactions, and the functions of the specific domains present in the carboxyl terminus (COOH terminus). The amino-terminal motor domain contains an ATP-sensitive F-actin-binding site and provides the force required for movement along actin filaments. The COOH-terminal tail region of MYOA is composed of an IQ domain with two IQ motifs, a TH-1-like domain, an SH3 domain, and a proline/alanine-rich domain with 2 proline/alanine motifs (Fig. 1). The TH-1-like domain can be further subdivided into 2 subdomains. The first subdomain is rich in basic amino acids and the second subdomain is slightly proline-rich.

We previously showed that MYOA plays a role in secretion and polarized growth by the creation of a conditionally null *myoA* strain, CL3, in which the inducible alcohol dehydrogenase (*alcA*) promoter drives the expression of *myoA* (9). More recently, we demonstrated that MYOA functions in endocytosis by mutating the phosphorylation site serine 371 to glutamic acid and activating endocytosis (10). Here we investigate the structural requirements of the tail region of MYOA that are necessary for its function. Transformation of the CL3 strain with mutant forms of *myoA* under the control of its own promoter allows us to selectively maintain an otherwise lethal transformant for further study. The use of an inducible promoter to produce wild type MYOA and the endogenous *myoA* promoter to produce mutant MYOA allows for differential expression of either the wild type or mutant MYOA or both depending on the growth medium.

This paper addresses the *in vivo* significance of the four domains present in the COOH-terminal region of MYOA. We have chosen to mutate the tail domains of *myoA* because it is this portion of the polypeptide that leads to specific cellular localization and function. We have transformed six different mutant tail constructs corresponding to frameshift and deletion mutations and tested them for their ability to complement the conditional null phenotype of CL3. Additionally, we have characterized the phenotypes of the viable *myoA* frameshift and deletion mutants by examining the consequences of these changes on cell growth, cell morphology, protein secretion, and endocytosis.

MATERIALS AND METHODS

Strains, Media, and Growth Conditions—Construction of the CL3 strain was described previously (9). The yeast strain Y190 (*MAT*a *gal4*Δ, *gal80*Δ, *his3*Δ*200, trp1-901, ade2-101, ura3-52, leu2-3, 112, URA3::GAL→lacZ, LYS2::GAL(UAS)→HIS3, cyh*^{r}) was used for two-hybrid screens (11). The bacterial strain DH5αF′ [F′ ϕ80d*lac*ZΔM15 Δ(*lac*ZYA-*arg*F)U169 *deo*R *rec*A1 *end*A1 *hsd*R17(r_k^-, mk^+) *sup*E44 λ$^-$

* This work was supported by grants from the National Institutes of Health, NIGMS (to G. S. M.) and a National Institutes of Health training grant (to R. A. Y.). The costs of publication of this article were defrayed in part by the payment of page charges. This article must therefore be hereby marked "*advertisement*" in accordance with 18 U.S.C. Section 1734 solely to indicate this fact.

‡ Contributed equally to the results of this work.

§ To whom all correspondence should be addressed: Dept. of Cell Biology, Baylor College of Medicine, One Baylor Plaza, Houston, TX 77030. Tel.: 713-798-4756; Fax: 713-798-7799; E-mail: gsmay@bcm.tmc.edu.

[1] The abbreviations used are: TH, tail homology; SH3, Src homology 3; CL3, conditional lethal clone 3; YAG, yeast extract glucose; kb, kilobase(s); PCR, polymerase chain reaction; MM, minimal medium; PAGE, polyacrylamide gel electrophoresis.

TABLE I
Plasmids used in these studies

Strain	Vector	Marker	Insert
pGEM*myoAKpn*I	pGEM*myoA*		MYOA 1–744
pGEM*myoAXho*I	pGEM*myoA*		MYOA 1–1126
pGEM*myoABam*HI	pGEM*myoA*		MYOA 1–1155
FSK*pn*I	pGEM*myoA*	*pyroA*	MYOA 1–744
FS*Xho*I	pGEM*myoA*	*pyroA*	MYOA 1–1126
FSB*am*HI	pGEM*myoA*	*pyroA*	MYOA 1–1155
pBKSΔIQ	pBluescriptKS		MYOA1–730, 793–1160
pBKSΔTH-1-like	pBluescriptKS		MYOA1–792, 1081–1160
pBKSΔSH3	pBluescriptKS		MYOA1–1080, 1131–1160
pGEM*myoA*ΔIQ	pGEM*myoA*		MYOA1–730, 793–1160
pGEM*myoA*ΔTH-1-like	pGEM*myoA*		MYOA1–792, 1081–1160
pGEM*myoA*ΔSH3	pGEM*myoA*		MYOA1–1080, 1131–1160
ΔIQ	pGEM*myoA*	*pyroA*	MYOA1–730, 793–1160
ΔTH-1-like	pGEM*myoA*	*pyroA*	MYOA1–792, 1081–1160
ΔSH3	pGEM*myoA*	*pyroA*	MYOA1–1080, 1131–1160
p*myoA*9	pUC19		MYOA 731–1249
p*myoA*10	PAS2	*TRP1*	MYOA 731–1249
p*myoA*11	pUC19		MYOA 793–1249
p*myoA*12	pUC19		MYOA 1081–1249
p*myoA*13	PAS2	*TRP1*	MYOA 793–1249
pmyoA14	PAS2	*TRP1*	MYOA 1081–1249
p*myoA*18	PRSETA		MYOA 731–1249
p*myoA*19	PRSETA		MYOA 793–1249
p*myoA*20	PRSETA		MYOA 1081–1249

thi-1 *gyr*A96 *rel*A1] was used for routine propagation of plasmids. *Aspergillus* media used were yeast extract glucose (YAG) medium and minimal medium with either 1% dextrose (MM-glucose) or 0.1% glycerol (MM-glycerol) as described previously (9). MMV-glycerol contains MM-glycerol with vitamin mixture (12).

Mutagenesis—A pGEM plasmid, pGEM*myoA*, which contains an 8.7-kb *Xba*I to *Sac*I genomic fragment of the *myoA* gene with its native promoter and termination sequence, was used to create the tail mutants (Table I). Frameshift mutations were made by cutting pGEM-*myoA* with *Kpn*I, *Xho*I, or *Bam*HI enzyme. pGEM*myoAKpn*I was made blunt with T4 polymerase and pGEM*myoAXho*I and pGEM*myoA-Bam*HI were made blunt with Klenow enzyme and religated according to the protocols of the supplier (New England Biolabs, Beverly, MA). These frameshifts truncated MYOA at amino acid positions 744 (*Kpn*I), 1126 (*Xho*I), and 1155 (*Bam*HI). The changes these mutations make to the sequence are shown in Fig. 1*B*. *pyroA,* a selective marker for transformation, was cloned as an *Sph*I-*Spe*I fragment into the *Sph*I-*Xba*I site of each of the *myoA* mutant constructs. These constructs were renamed FS*Kpn*I, FS*Xho*I, and FS*Bam*HI, respectively (Table I). FS*Kpn*I causes a frameshift in the middle of the IQ domain, essentially producing MYOA without a tail. FS*Xho*I results in a frameshift after the SH3 domain producing MYOA without a proline-rich region (amino acids 1138–1147). FS*Bam*HI causes a frameshift after the first of two proline-rich motifs found in MYOA, producing a protein that lacks the last proline-rich motif.

The IQ, TH-1-like, and SH3 deletion mutations were created using a PCR based mutagenesis method (13). The deleted regions were defined as follows: the IQ domain (amino acids 731–792), the TH-1-like domain (amino acids 793–1080), and the SH3 domain (amino acids 1081–1130) (Fig. 1). The oligonucleotide sequences and the primer pairs for each template used are given in Tables II and III, respectively. Plasmid pBKS *Spe*I-*Bam*HI (pBluescript KS, Stratagene) which contains a *Spe*I-*Bam*HI fragment of *myoA* was used as the template. Primer pairs listed in Table III were used to generate two initial PCR products for each deletion, which were subsequently used to prime themselves in a third PCR reaction to create the full-length deletions. The final PCR product was cloned as an *Eag*I-*Bam*HI replacement fragment into pBKS *Spe*I-*Bam*HI.

The presence of the specific mutations and the absence of other changes were confirmed by DNA sequencing. The deletion mutants in pBKS *Spe*I-BamHI fragments were used to replace the equivalent wild type sequences of parental pGEM*myoA* and *pyroA* was added as described above. pGEM*myoA,* pGEM*myoA*ΔIQ, pGEM*myoA*ΔTH-1-like, and pGEM*myoA*ΔSH3 were renamed CL3-WT, ΔIQ, ΔTH-1-like, and ΔSH3 (Table I).

Plasmids containing the different frameshift or deletion mutations were transformed into CL3. Primary transformants were purified three times to single spores on selective MM-glycerol medium. Southern analysis was used to identify transformants containing a single integration at the *myoA*Δ locus in CL3 upstream of the *myoA* driven by the *alcA* promoter.

Southern Analysis—Cultures of all transformants were grown in MM-glycerol liquid to allow for growth by permitting expression of the *alcA* wild type *myoA* gene. Genomic DNA was isolated as described previously (14). The genomic DNAs were digested with *Xho*I and probed sequentially with the 0.9-kb *Hin*dIII-XhoI 3′ half of *pyroA*, the 1-kb *Xho*I-EcoRI 5′ half of *pyroA*, and the *Eco*RI *pyr-4* fragment, radiolabeled using the random primer method (15). Hybridization conditions were those described previously (16).

Protein Gel Electrophoresis and Western Analysis—Cultures of all transformants were grown in either liquid YAG or MM-glycerol, harvested, and pressed dry between paper towels. The cell mass was pulverized in a Dounce homogenizer and suspended in 10% trichloroacetic acid. After incubation for 5 min at room temperature, the pellet was washed twice in acetone with 20 mM HCl and once in acetone. The cell mass was suspended in 8 M urea made in SDS sample buffer (17) and boiled for 5 min. The extract was centrifuged for 15 min at 15,000 rpm to remove the insoluble cell debris and 20 μg of total cellular proteins were separated on a 6% SDS-PAGE. The proteins were transferred to a nitrocellulose membrane (Schleicher and Schuell, Keene, NH) by electroblotting. MYOA proteins were detected using an affinity purified polyclonal MYOA antibody raised against the COOH-terminal portion of MYOA expressed in *Escherichia coli* using the PRSET expression system (9). Peroxidase-conjugated goat anti-rabbit antibody was used as the secondary antibody. Chemiluminescent detection of the proteins by ECL (Amersham Corp.) was used to verify the presence of the various MYOA mutant proteins.

Growth Studies—Induction or repression of the *alcA* promoter was demonstrated by plating the transformants on various carbon sources (9). Growth in YAG represses the *alcA* driven *myoA* and allows the endogenous *myoA* promoter to transcribe the mutated MYOA product, such that if the portion of the tail deleted is an essential region for myosin I function, a lethal phenotype would be expected. Growth on MM-glycerol medium induces the *alcA* driven *myoA*, such that wild type MYOA is produced and all strains will be viable and wild type for growth.

Hyphal growth studies were performed by plating 10^4-10^6 spores/ml onto sterile coverslips in YAG. At various time points a coverslip was removed randomly selected samples were chosen and recorded. The lengths of the germlings were measured in microns. Recorded images were also analyzed for germination and branching morphology. Radial growth assays were performed by plating 2–3 colony forming units per plate on solid YAG as described previously (16).

Microscopy—Spores were germinated in YAG for differential interference contrast microscopy. Germ tube development observed using a Nikon microscope and digital images were collected at 1-h intervals using a Hamamatsu Model C2400 camera using a SCSI adapter and twain driver into Adobe Photoshop 3.0.

Two-hybrid Screen—To make the bait plasmids an *Nde*I site was introduced by oligonucleotide-directed mutagenesis of the *myoA* cDNA (9) introducing an in-frame methionine at amino acid positions 724, 792, or 1079 of the MYOA protein corresponding to the IQ, TH-1-like, and SH3 domains. The PCR fragments were then cloned into the *Nde*I and *Xba*I sites in pUC19 before being cloned into pAS2 as *Nde*I-*Sal*I fragments. The *A. nidulans* activation domain library was constructed in pAD-GAL4 (Stratagene, La Jolla, CA) and was kindly provided by Dr. Osmani of the Geisinger Clinic, Weis Center for Research, Danville, PA. The two-hybrid screen was conducted as described (11).

Binding of MYOA to CaM-Sepharose—The same cDNA fragments in pUC19 used to make the bait plasmids were cloned into PRSETA (Invitrogen, Carlsbad, CA) vector that had *Nde*I and *Hin*dIII sites. These plasmids were used in a linked *in vitro* transcription/translation reaction (PROTEINscript, Ambion, Inc., Austin, TX) and the translated product was used in a direct binding assay to CaM-Sepharose (P4385, Sigma) in 50 mM Tris-HCl, pH 8.0, 150 mM NaCl with 1 mM CaCl or with 1 mM EGTA. The CaM-Sepharose slurry was incubated with the different translation products in the two buffers for 30 min at 4° C with gentle mixing. The CaM-Sepharose beads were washed three times with buffer and examined on 10% SDS-PAGE (17) with starting material as a control for amount of protein present. Following electrophoresis the proteins were stained with Coomassie Blue, dried, and exposed to x-ray film at −70 °C.

Genetic, Molecular Genetic and Other Methods—Methods for the growth and genetic manipulation of *A. nidulans* have been described in detail elsewhere (12, 18). Similarly, those methods used in the manipulation of plasmids and molecular cloning have been described elsewhere (18).

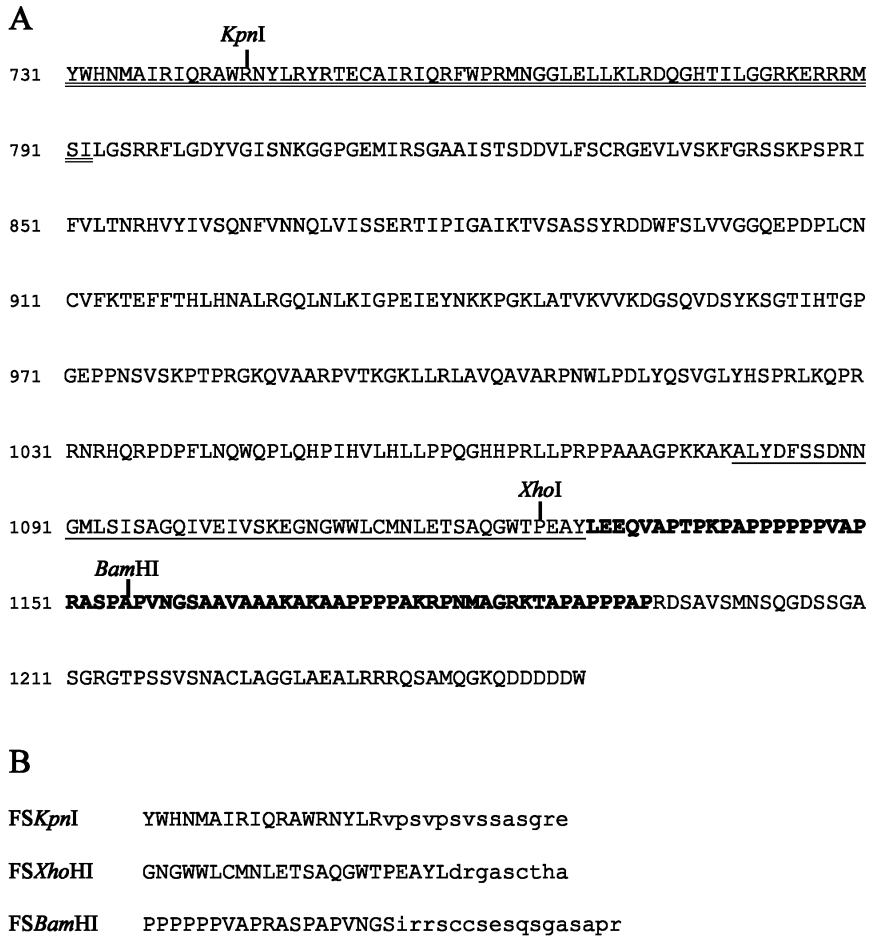

FIG. 1. *A,* protein sequence of the tail region of MYOA showing the different domains. The IQ domain is *double underlined*, the SH3 domain is *underlined*, the proline-rich region is in *bold* and the TH-1-like domain is the sequence between the IQ and SH3 domains. The positions of the restriction endonuclease cleavage sites used to make frameshift mutants are indicated *above* the amino acid sequences. *B,* sequence changes caused by each of the frameshift mutations, with newly added amino acids in *lowercase*.

TABLE II
Oligonucleotides used in these studies and their sequences

Primer	Sequence
*myoA*4	GAACCATTAAGCCTA
T3	ATTAACCCTCACTAAAG
IQ-1	GAGGCTATGCGCGACCGCCTTGGTTCTCGACGGTTC
IQ-2	GAACCGTCGAGAACCAAGGCGGTCGCGCATAGCCTC
TH-1-like-1	CGTAGGAGAATGAGCATTGCCCTGTACGACTTCAGC
TH-1-like-2	GCTGAAGTCGTACAGGGCAATGCTCATTCTCCTACG
SH3–1	GGACCGAAGAAAGCAAAGGAGGAGCAAGTTGCACCC
SH3–2	GGGTGCAACTTGCTCCTCCTTTGCTTTCTTCGGTCC

TABLE III
Oligonucleotide primer pairs and the templates used to make the PCR products in the construction of the MYOA deletion mutants

Template	Primer pairs	Predicted size
		bp
pBKS *Spe*I-*Bam*HI	IQ-1/T3	1100
pBKS *Spe*I-*Bam*HI	*myoA*4/IQ-2	330
pBKS *Spe*I-*Bam*HI	TH-1-like-1/T3	240
pBKS *Spe*I-*Bam*HI	*myoA*4/TH-1-like-2	600
pBKS *Spe*I-*Bam*HI	SH3–1/T3	80
pBKS *Spe*I-*Bam*HI	*myoA*4/SH3–2	1390
IQ PCR products	*myoA*4/T3	1400
TH-1-like PCR products	*myoA*4/T3	770
SH3 PCR products	*myoA*4/T3	1470

RESULTS

Detection of the myoA Frameshift and Deletion Mutations in the Genome—It is the tail region of class I myosins that is thought to provide them with their specific cellular location and function. For this reason we began our mutational studies of class I myosin function in *A. nidulans* by creating frameshift and deletion mutants that would alter specific domains of the polypeptide. Our emphasis in these studies was on the highly conserved IQ, calmodulin binding motif, the SH3 domain, and the proline-rich region of the polypeptide. Genomic Southern analysis was performed on 15 purified transformants for each of the transforming plasmids. Genomic DNA digested with *Xho*I was probed with 3 different probes to identify integration into the *myoA*Δ locus (Figs. 2 and 3). Approximately 70% of transformants had integrated a single copy of the mutant allele into the *alcA* activated full-length *myoA* locus, and these were discarded because of the probability of interallelic recombination between the mutant and wild type tail domains. Only 20% of the transformants had integrated a single copy of the mutant allele into the shorter *myoA*Δ locus (Figs. 2 and 3). These were selected for further study. Surprisingly, the TH-1-like mutant integrated only into the *alcA-myoA* gene, so these transformants were mapped to verify that recombination had not occurred between wild type and mutant alleles and selected for further study (Fig. 3, *lane 7*). The phenotypes of the frameshift and deletion mutations were confirmed for at least three independent isolates.

The Mutant MYOA Proteins Are Detected by Western Blotting—Mutant strains were grown on MM-glycerol medium so that both the wild type MYOA protein, whose synthesis was driven by the *alcA* promoter and the mutant MYOA protein made from the *myoA* promoter were expressed. In addition, viable mutant strains were grown on rich YAG medium to repress expression of the wild type protein. The CL3 and CL3-WT transformant control strains (Fig. 4) demonstrate that under repressing growth conditions (Fig. 4, *lanes labeled Y*) CL3 expresses barely detectable levels of wild type MYOA. The results indicate that the mutant proteins are expressed for the FS*BamHI*, ΔIQ, ΔTH-1-like, and ΔSH3 strains (*lanes labeled Y*

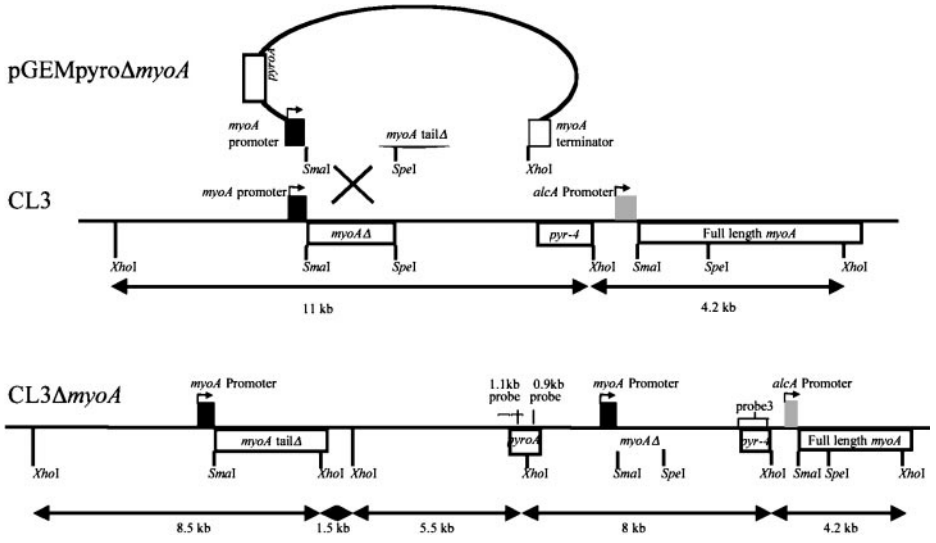

FIG. 2. **Map for expected integration of pGEM*myoA* frameshift and tail mutations into the *myoA*Δ locus of CL3 and the predicted restriction polymorphism of the mutant gene from the expressed locus.** Predicted sizes of genomic fragments when digested with *Xho*I are shown. Probes from *pyro*A and *pyr*-4 were used to confirm the correct integration.

show the mutant MYOA and the *G lanes* show both the wild type and mutant MYOA). Distinguishing between the presence of the FS*Xho*I mutant protein and the wild type MYOA protein in MM-glycerol was difficult because the antibody reacts only weakly with the mutant protein due to deletion of a portion of the tail recognized by the antibody. However, the FS*Xho*I MYOA mutant protein was clearly identified when the strain was grown in YAG. The FS*Kpn*I mutant protein could not be detected because it lacks the portion of the tail domain recognized by our antibody. Protein loaded on each lane was approximately equal as demonstrated by a nonspecific lower molecular weight band (labeled *NS*) present in every lane.

Growth Characteristics of the FSXhoI, FSBamHI, ΔIQ, and ΔSH3 Mutants—We examined the growth of control and mutant strains on solid and liquid media to assess the phenotypes of the various *myoA* mutations used in this study. Growth was assessed on liquid as well as solid media because we previously have seen defects in submerged culture not seen on solid media (10). Growth of the mutant strains, a wild type *myoA* control transformant, and the parental CL3 strain was tested on solid YAG and MMV-glycerol plates to determine the effect of the mutations on their ability to form a colony (Fig. 5). As expected for recessive mutations, all the strains exhibited wild type growth on MMV-glycerol medium because as shown by Western blotting, both the mutant and wild type MYOA proteins are made when the fungus is grown on this medium (Fig. 5, *A* and *B*). On YAG medium the FS*Bam*HI and ΔSH3 strains appeared to grow as well as the wild type control and in quantitative growth studies, we found the FS*Bam*HI and ΔSH3 strains produced colonies that were 96 and 86%, respectively, of the CL3-WT strain in diameter. In contrast, the ΔIQ and FS*Xho*I mutants formed very small colonies on YAG (Fig. 5, *c* and *d*), while the FS*Kpn*I and ΔTH-1-like mutants did not grow at all. The differential growth effect for the mutants on YAG is because the *alcA* promoter is repressed, thus allowing only the mutant form of MYOA to be expressed. We next examined the growth of the control and mutant strains in submerged culture.

The processes of spore germination, germ tube emergence, hyphal branching, and septation are precisely controlled events in *A. nidulans* (19, 20). For wild type strains the first visible sign of spore germination is spore swelling at about 2 h of growth, followed by germ tube emergence at 5–7 h (Table IV and Fig. 6). There is then a period of rapid hyphal growth by apical extension. Between 8 and 10 h of growth a second germ tube emerges from the swollen spore on the side opposite of where the first germ tube emerged. After 11 to 12 h of growth, hyphal branches begin to appear from the subapical compartments of the growing mycelium. With these observations as our baseline, we assessed each of the mutants for defects in these processes (Table IV, Fig. 6). The FS*Bam*HI and ΔSH3 mutant strains begin to germinate at 6–7 h with only a slight delay in reaching the maximum compared with the wild type control and hyphal elongation was at a rate similar to that of the control strain (Fig. 6). In contrast, the ΔIQ and FS*Xho*I mutants germinate much later, only after 10 or more hours in culture and their rate of hyphal growth is greatly reduced (Fig. 6). During the first 8 h of growth the ΔIQ and FS*Xho*I mutants display only isotropic growth like that seen for the parental CL3 strain (Fig. 7). In contrast, the control, ΔSH3, and FS*Bam*HI mutant strains all germinated (80–90% of the spores, Table IV) and extended germ tubes that produced normal hyphae (Fig. 7). The viable mutants all displayed reduced hyphal growth rates compared with controls in submerged cultures. The ΔIQ mutant displayed the slowest rate of hyphal elongation at 16% of the wild type rate. The FS*Xho*I had a hyphal growth rate that was 36% of wild type. The FS*Bam*HI and ΔSH3 mutants had hyphal growth rates that were 64 and 54% that of the wild type rate, respectively. Thus, while these two mutants display only slightly reduced rates of radial growth on plates they grew significantly slower in submerged culture, like we previously saw for other *myoA* mutations (10).

The FSXhoI and ΔSH3 Mutants Have Defects in Septation and Hyphal Morphogenesis—We examined the growth of the ΔIQ and the FS*Xho*I mutant strains in greater detail because of their dramatic growth defects (Fig. 8). The ΔIQ mutant strain began germination after 9–10 h, approximately 3–4 h later than the CL3-WT strain. In 5–10% of the population, ΔIQ more than one germ tube emerged and in some cases up to 5 germ tubes appeared simultaneously from the swollen spore. Furthermore, in 90% of the germlings a second germ tube appeared at an odd angle, instead of emerging on the side opposite the first germtube as in the wild type control. The ΔIQ mutant strain produced hyphae that were contorted and kinked with visibly thickened cell walls. The average diameter of the hyphae was approximately twice that of the control strain (Table V). Multiple hyphal branches from a single subapical compartment were frequently observed and the branches were perpendicular rather than the acute angle seen in the wild type. Septa were also irregularly spaced and were often formed at odd angles (Fig. 8). Septa were placed every 16 ± 7 μm compared with the 39 ± 5 μm in the wild type control hyphae (Table V).

The FS*Xho*I mutant began germinating after 10 h, nearly 5 h

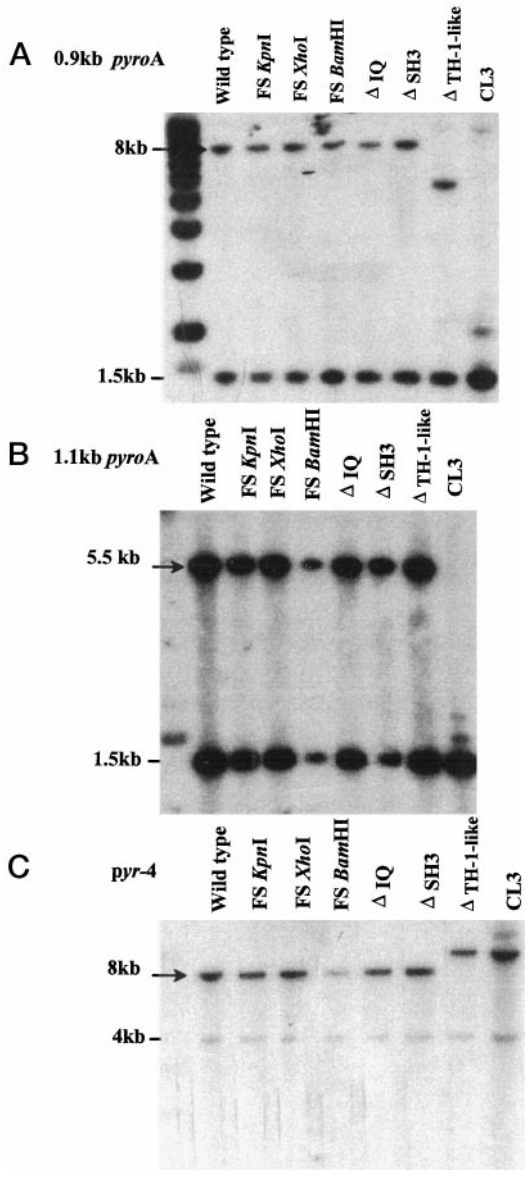

FIG. 3. **Southern blot of CL3, CL3-WT, and tail mutant strains.** Genomic DNA was digested with *Xho*I and sequentially probed with (*A*) the 0.9-kb *pyroA* fragment (*B*) 1.1-kb *pyroA* fragment, and (*C*) *pyr-4*. *Arrows* indicate expected bands corresponding to a single homologous integration into the *myoA*Δ site of the CL3 strain. The 1.5-kb band is from the endogenous *pyro*A gene. The *pyr*-4 probe also weakly hybridizes to a 4-kb *Xho*I fragment downstream of the 8-kb fragment that contains a short *pyr-4* sequence.

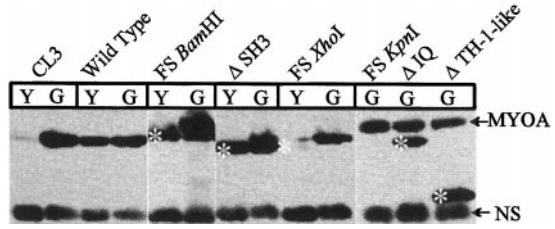

FIG. 4. **Western blot of CL3, CL3-WT, and tail mutant strains grown on MM-glycerol (*lanes G*) and YAG (*lanes Y*).** Strains were grown in either YAG, in which repression of the *alcA* promoter allows for only mutant MYOA to be expressed, or MM-glycerol in which both wild type and mutant MYOA are expressed. Predicted sizes of mutant proteins are: CL3-WT (138 kDa), FS*Kpn*I (79 kDa), FS*Xho*I (125 kDa), FS*Bam*HI (129 kDa), ΔIQ (129 kDa), ΔTH-1-like (101 kDa), and ΔSH3 (132 kDa). The *arrow* indicates the wild type MYOA and the *asterisks* indicate the mutant MYOA that corresponds to their predicted sizes. The unidentified band below is nonspecific (*NS*) and was used as an indication of protein loading. The FS*Bam*HI lanes were taken from another gel.

after CL3-WT. FS*Xho*I germlings display aberrant hyphal branching pattern that is distinct from the hyphal branching defects seen in the ΔIQ mutant. In the FS*Xho*I mutant Y-shaped apical compartments (Fig. 8) characterize the hyphal branching defect. Branches in the apical compartment of wild type hyphae are never observed. Hyphal and septal morphology are structurally normal in this mutant (Fig. 8), although the positioning of septa is abnormal. Septa were spaced every 18 ± 6 μm in the FS*Xho*I mutant compared with 39 ± 5 μm in the control strain (Table V).

Decreased Levels of Wild Type MYOA Results in Phenotypic Growth Defects That Are Distinct from the Mutant Strains—There are two ways to explain the spectrum of phenotypes found in the MYOA tail domain mutants. The first is that they simply reflect the general level of activity of each mutant MYOA, from inactive (FS*Kpn*I, ΔTH-1-like) through partially active (ΔIQ, FS*Xho*I) to almost normal (ΔSH3 and FS*Bam*HI). The second is that the phenotype of each mutant reflects a subset of defects correlating with the specific role of the deleted domain, thereby providing us with insight into their function. In order to test these hypotheses, wild type MYOA was expressed at different levels in the CL3 strain, and the phenotypes were examined in detail. Expression of MYOA under the control of the *alcA* promoter can be controlled in the CL3 strain by the choice of the growth medium (9). The CL3 strain was grown on repressing medium (YAG), semi-repressing medium (MM-glucose), and nonrepressing, noninducing medium (MM-glycerol) to assess the *in vivo* effects of the levels of MYOA expression on the growth of the fungus. Previously, a Western blot of the CL3 strain grown on the various carbon sources and probed with an affinity purified MYOA antibody was used to demonstrate that growth on these different media resulted in differing levels of MYOA (9) and these differing levels give rise to different phenotypes (Fig. 9). On YAG little or no MYOA is being expressed and results in isotropic growth. On MM-glucose small quantities of MYOA are produced resulting in initial isotropic growth, thickened cell walls, perpendicular hyphal branching, decreased septal spacing, and swellings throughout the germ tube and septal walls. In contrast, the FS*Xho*I mutant displays a very different phenotype, with normal cell wall thickness, septal compartments that are shorter and septal walls that are perpendicular to the hyphal compartments. The ΔIQ mutant differs from the CL3 on MM-glucose in that its septa are not perpendicular to the germ tube and they are present more frequently. We concluded therefore that the phenotypes of the tail domain mutants do not simply reflect the levels of functional MYOA present and provide us with insights into how the different domains contribute to MYOA function *in vivo*.

CaM Binds to the IQ Motif of MYOA—As a means of understanding why the deletion of the IQ domain or the proline-rich domain was deleterious to the growth of the fungus, we undertook a study to identify proteins that interact with the tail region of MYOA. Using the entire tail region of MYOA as bait, p*myoA*10 (Table I), in a two-hybrid screen, we isolated 82 positive clones that interacted with the tail region of MYOA. All but one of these MYOA interacting clones encoded calmodulin (CaM). It had been shown previously that CaM or other EF-hand proteins serve as the light chain for class I myosins (1, 2). None of the CaM encoding clones were positive in the two-hybrid analysis with bait clones p*myoA*13 and p*myoA*14 (Table I) that lacked the IQ motifs, implicating the IQ motifs for the site of interaction for CaM. The same coding regions were cloned into PRSETA generating p*myoA*18, p*myoA* 19, and

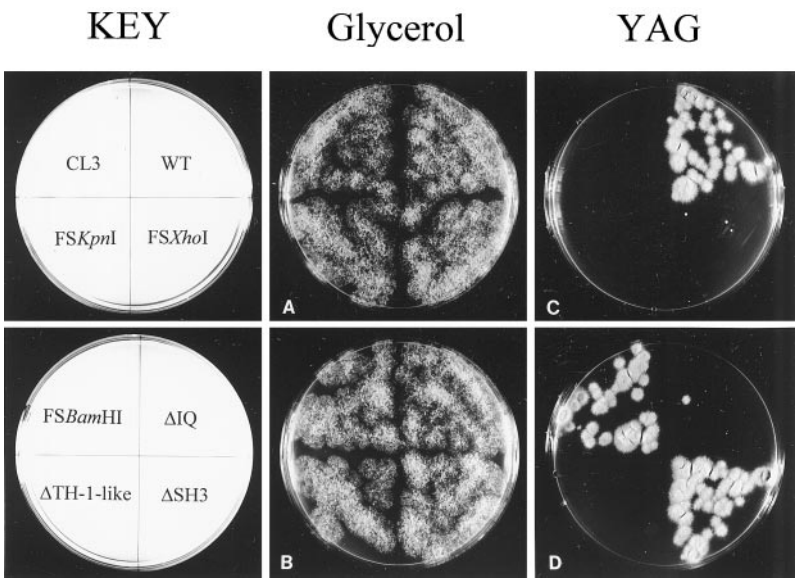

FIG. 5. **Growth of CL3 and CL3 transformants on repressing medium (YAG) or nonrepressing medium (glycerol).** Expression of MYOA under the control of the *alcA* promoter can be controlled in the CL3 strain and in its derivatives by the choice of growth medium. Strains were streaked out on MMV-glycerol (*A* and *B*) and YAG (*C* and *D*) to determine if the mutants produced a functional MYOA protein. FS*Bam*HI and ΔSH3 grow like the wild type MYOA transformant, CL3-WT, while FS*Xho*I and ΔIQ form tiny colonies. FS*Kpn*I and ΔTH-1-like fail to complement the conditional null of the CL3 strain.

TABLE IV
Germination and growth phenotype of the mutants and a control showing slight delays (FSBamHI and ΔSH3) and long delays (FSXhoI and ΔIQ) in germination

Parental strain CL3 and transformed strains FSK*pnI* and ΔTH-1-like did not germinate during the time course of the experiment. Data are based on examination of 100 cells.

		Spore	Single germ tube	Multiple germ tubes	Branched mycelium
5 h	WT	98	2	0	0
	FS*Xho*I	99	1	0	0
	FS*Bam*HI	97	3	0	0
	ΔIQ	100	0	0	0
	ΔSH3	99	1	0	0
6 h	WT	77	23	0	0
	FS*Xho*I	99	1	0	0
	FS*Bam*HI	84	15	0	0
	ΔIQ	100	0	0	0
	ΔSH3	92	8	0	0
7 h	WT	25	70	0	0
	FS*Xho*I	98	2	0	0
	FS*Bam*HI	20	77	3	0
	ΔIQ	100	0	0	0
	ΔSH3	56	43	1	0
8 h	WT	6	89	5	0
	FS*Xho*I	99	1	6	0
	FS*Bam*HI	18	76	6	0
	ΔIQ	99	1	0	0
	ΔSH3	18	77	5	0
9 h	WT	0	93	7	0
	FS*Xho*I	98	2	0	0
	FS*Bam*HI	3	90	7	0
	ΔIQ	90	3	7	0
	ΔSH3	1	94	5	0
10 h	WT	0	94	5	1
	FS*Xho*I	98	2	0	0
	FS*Bam*HI	1	83	16	0
	ΔIQ	40	5	55	0
	ΔSH3	0	85	15	0
11 h	WT	0	91	7	2
	FS*Xho*I	38	56	6	0
	FS*Bam*HI	0	90	9	1
	ΔIQ	1	12	78	0
	ΔSH3	1	86	13	0

p*myoA* 20 (Table III) for *in vitro* transcription and translation. The products of the reaction were used for CaM-Sepharose affinity chromatography. Only the longest protein containing the IQ motifs bound to CaM-Sepharose in the presence of

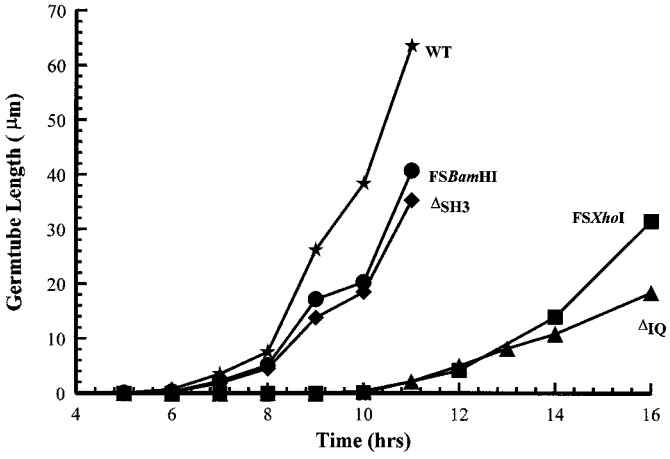

FIG. 6. **Growth curves for CL3-WT, FS*Xho*I, FS*Bam*HI, ΔIQ, and ΔSH3.** Strains were germinated in liquid YAG and hyphal length was measured as a function of time. Parental strain CL3 and transformed strains FS*Kpn*I and ΔTH-1-like were not included in this experiment because they do not form hyphae.

EGTA and Ca^{2+} (Fig. 10, p*myoA*18 lanes). Both the two-hybrid system and the CaM-Sepharose binding assay mapped the CaM-binding site to a 62-amino acid region that consists of a known CaM-binding structure, the IQ motif.

DISCUSSION

Our experiments address the *in vivo* structural requirements of the tail region of the class I myosin, MYOA. The mutations we have made result in three phenotypes. First are those mutations that result in a limited but measurable effect on MYOA function, like the ΔSH3 and FS*Bam*HI mutations. The second are those mutations that lead to a complete loss of MYOA function and include the ΔTH-1-like and the FS*Kpn*I mutants. The last class of mutations are those that have a profound impact on MYOA function. These are the ΔIQ and FS*Xho*I mutations.

To our surprise, the ΔSH3 mutation had a minimal effect on MYOA function. In other proteins, the SH3 and proline-rich domains have been shown to mediate protein-protein interactions (3) and in fact, proline-rich motifs have been shown to directly interact with the SH3 domains (21). In MYOA, however, deletion of the SH3 domain led to nearly wild type growth. Therefore, if SH3 is mediating some protein-protein interaction in our system it is not essential or it is redundant with another

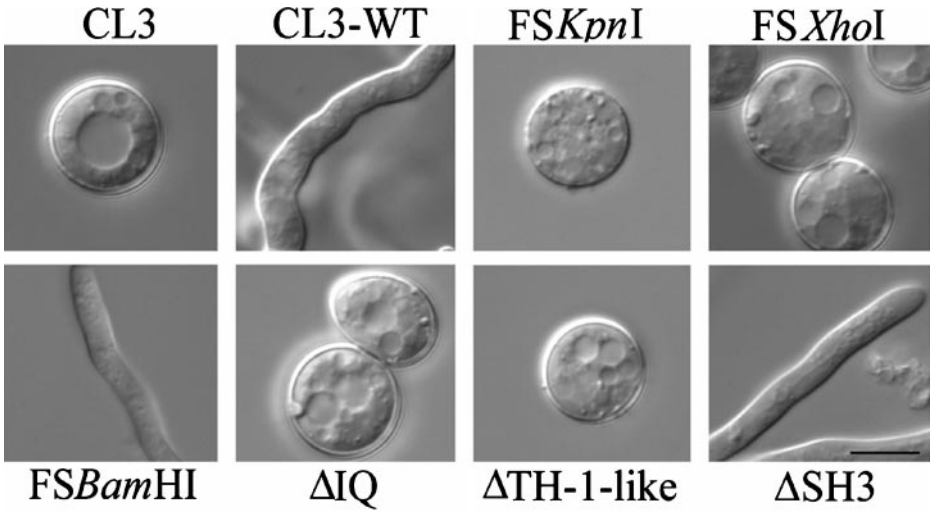

FIG. 7. **Differential interference contrast micrographs of the controls and mutants after 8 h at 37 °C.** *Bar* represents 5 μm.

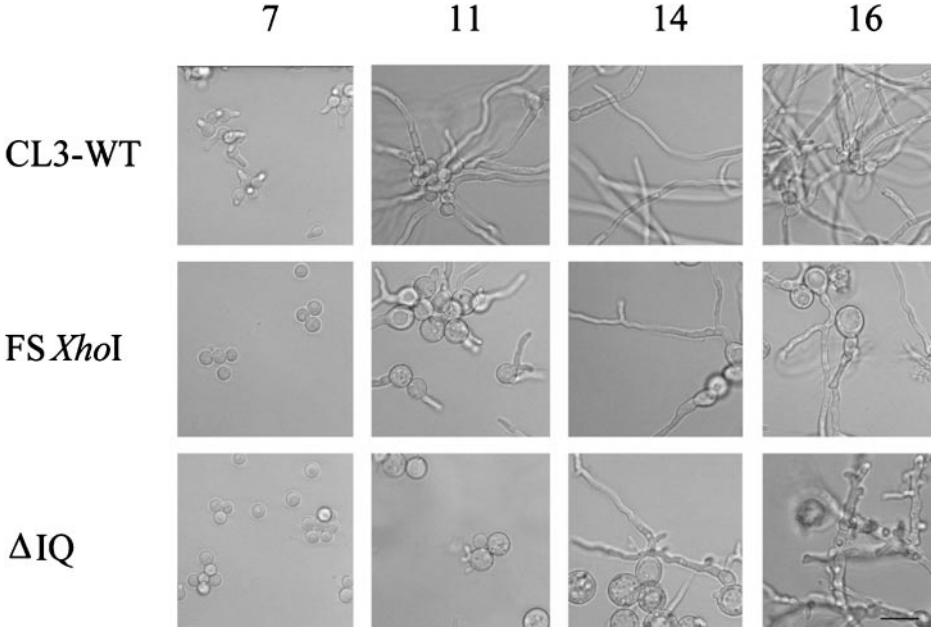

FIG. 8. **Hyphal growth phenotypes for FS*Xho*I and ΔIQ mutants compared with the control strain CL3-WT.** Phase micrographs were made at intervals during growth in liquid YAG. The time in hours is indicated at the *top* of each column. Both the FS*Xho*I and ΔIQ mutants germinate at 11 h and produce multiple germ tubes from the same spore simultaneously. In addition, the FS*Xho*I mutant also displays abnormal hyphal branching which produces Y-shaped apical compartments at 14 and 16 h. In contrast, the ΔIQ mutant exhibits aberrant branching at right angles with multiple sites of initiation in a single compartment. Hyphal tips and compartments are also swollen with thickened cell walls. *Bar* represents 10 μm.

TABLE V
Septal spacing and size of the sub apical hyphal compartments for the various mutants and the control, CL3-WT

The values are based on the averages of 50 compartments. Measurements are given in micrometers.

Strain	Width	Length
CL3-WT	1.8 ± 0	39 ± 5
FS*Bam*HI	1.8 ± 0	39 ± 6
ΔSH3	1.8 ± 0	39 ± 5
ΔIQ	3.9 ± 1.1	16 ± 7
FS*Xho*I	2.1 ± 0.5	13.5 ± 7

system that compensates for loss of the SH3 domain. However, removal of the entire proline-rich COOH-terminal domain, in the FS*Xho*I mutant, resulted in a mutant MYOA that retained only limited function. This mutant grew very poorly and displayed abnormal hyphal branching, suggestive of a failure to correctly initiate and maintain polar apical growth. This suggests that in our system, it is the proline-rich domain, and not the SH3 domain that makes the critically important protein-protein interaction. It is possible that the proline-rich and SH3 domains cooperate in mediating a specific protein interaction and that the SH3 domain acts to fine-tune this interaction. These interactions are possibly necessary for MYOA to be properly localized and thus play a significant role in preventing the precocious formation of hyphal branches. We hypothesize that the proline-rich domain plays an important role in maintaining MYOA at the growing hyphal tip and in the mutant there is a failure to maintain MYOA at a single site, leading to the formation of a second site of apical extension.

In addition, the FS*Bam*HI mutant defines the minimal proline-rich region required for MYOA function. The proline-rich domain consists of two parts with the *Bam*HI site residing in between the two motifs. It still remains to be seen whether a corollary to this mutant, namely one that has the second proline-rich motif will be the functional equivalent of the FS-*Bam*HI mutant. We hope to define the essential role of the proline-rich domain in MYOA by creating additional mutations in these domains and by identifying their interacting partners.

The ΔIQ mutation affects more cellular structures than the FS*Xho*I mutation. The variety of defects including thickened cell walls, shorter wider hyphal compartments, and multiple germ tubes seen in this mutant is difficult to explain in a simple model. The IQ motifs define the light chain-binding domain in other myosins. The myosin light chains are members of the EF-hand superfamily of proteins (22) and include the calcium-binding protein, CaM. We have shown that CaM is the light chain of MYOA like in many other myosins (23). The

FIG. 9. **Differential interference contrast micrographs of CL3 grown on different media for 11 h at 37 °C.** Expression of MYOA under the control of the *alcA* promoter can be controlled in the CL3 strain by the choice of medium. On YAG the *alcA* promoter is strongly repressed leading to almost no MYOA expression and subsequently only isotropic growth. On MMV-glucose the *alcA* promoter is somewhat leaky such that small amounts of MYOA are produced leading to thickened cell walls, perpendicular hyphal branching, and swellings throughout the germ tube. On MMV-glycerol the *alcA* promoter is not repressed leading to wild type expression of MYOA and normal wild type growth. *Bar* represents 10 μm.

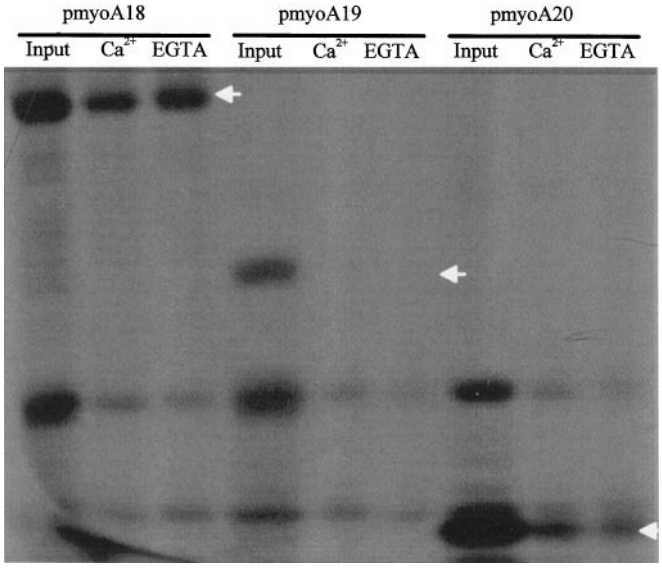

FIG. 10. **Binding *in vitro* translated proteins of MYOA to CaM-Sepharose.** Translated proteins corresponding to the entire tail, IQ-TH-1-like-SH3-Pro, or sequential deletions TH-1-like-SH3-Pro and SH3-Pro corresponding to p*myoA*18, 19, and 20, respectively, were tested for their binding to CaM-Sepharose in the presence of either 1 mM CaCl or 1 mM EGTA. Protein from p*myoA*18 which contains the IQ domain bound tightly to the CaM-Sepharose in the presence of EGTA or Ca^{2+}. This implies that the IQ domain directly interacts with CaM. The *arrows* indicate where the various truncated proteins run.

presence of calcium has also been shown to stimulate the actin-activated ATPase of other class I myosin 2–3-fold *in vitro* (24). Therefore, it is likely that *in vivo,* calcium plays a significant role in regulating MYOA and can partially explain the multiple cellular defects seen in the ΔIQ mutant. Additionally, the IQ domain is proposed to play a role in movement along the actin filament, functioning as a lever arm in the swinging cross-bridge model, in which the IQ motifs causes a conformational change in the head leading to a change in step size (25). This model predicts that removal of the IQ domain would lead to a reduced step size and thus a less effective myosin motor. We are currently producing the ΔIQ MYOA in a bacculovirus system for *in vitro* motility assays to test this hypothesis.

One way to explain the spectrum of phenotypes present in these studies is that they simply reflect the levels of functional MYOA present, ranging from a slightly impaired MYOA which leads to a mild phenotype to a severely impaired MYOA resulting in severe growth defects. An alternative to this hypothesis is that the different phenotypes provide us with insights into how the different domains contribute to MYOA function *in vivo*. Our analysis of the original conditional null mutant strain CL3 supports this alternative view. Since we are able to grow CL3 under a variety of conditions that will determine the amount of MYOA in the fungus, we are able to see how the levels of MYOA correlate with the cellular phenotype. When CL3 is grown on minimal glucose medium, the *alcA* promoter is not fully repressed as it is on yeast extract glucose medium. Under these conditions MYOA is made in limited quantities and the spectrum of cellular phenotypes we see are not identical to those seen in the ΔIQ or the FS*Xho*I mutants, as one would predict if the mutations were simply leading to a general loss of MYOA activity. Thus, the specific cellular defects we see in each of these mutants are a reflection of how MYOA is working in the hyphae.

Our previous work showed that MYOA was essential for viability and was required for polarized hyphal growth and protein secretion (9). In contrast, in budding yeast Myo5p has been shown to function in endocytosis but deletion of both class I myosin genes *MYO3* and *MYO5* is not a lethal event (6, 7). Our more recent work has also implicated MYOA in endocytosis in *A. nidulans* (10). Because of these studies, we also tested all the mutant strains with a variety of agents that perturb growth like the antimicrotubule agent benomyl. We also examined the mutants for defects in nuclear staining and localization (26), protein secretion (9), endocytosis (10, 27), and actin localization and found that they did not differ significantly from the control strain.

MYOA seems to be involved in several aspects of hyphal morphogenesis. It participates in endocytosis, as demonstrated by our studies of mutations at the TEDS site (10). MYOA also functions in septal wall formation, because the ΔIQ mutant shows defects in the positioning and orientation of septa. Additionally, MYOA plays a role in maintaining cell polarity, because the ΔIQ and FS*Xho*I mutants grown on YAG and the CL3 strain, when grown under conditions of limited MYOA expression (MMV-glucose) produce hyphae with abnormal branching patterns. Furthermore, the FS*Xho*I mutant can also form a branch in the apical compartment, something never seen in the wild type strain. Finally, MYOA has other roles in hyphal morphogenesis as illustrated by the abnormal hyphae made in the ΔIQ mutant, which produces contorted hyphae and displays swelling at hyphal tips and walls of subapical compartments. Thus, unlike the case in budding yeast where class I myosin activity is not absolutely required for cell growth, class I myosin function in the filamentous fungus *A. nidulans* is involved in a variety of activities, all of which contribute to the ability of the fungus to grow.

In summary, we have begun to determine *in vivo* the functional importance of the various domains in the tail region using in-frame deletion and frameshift mutations. Remarkably, the highly conserved SH3 domain could be removed from the protein with only minimal effects on MYOA function. In contrast, loss of the entire COOH-terminal proline-rich domain had a profound impact on MYOA function. Similarly, removal of the CaM-binding IQ domain resulted in a MYOA that had only a limited capacity to support hyphal growth. The observed

differences in cellular defects between the FS*Xho*I and ΔIQ mutations have allowed us to begin determining how the various domains contribute to the overall function of MYOA. We now need to determine how these important domains specifically contribute to the functioning of MYOA. More detailed studies of the effects of these and additional mutations on MYOA localization are currently in progress. In this respect, it is unfortunate that our antibody detects proteins other than MYOA on Western blots precluding its use in immunoflouresscence localization studies of the mutant proteins. We are also trying to identify the proteins that MYOA interacts with to better understand how these complexes mediate the various activities of MYOA.

Acknowledgments—We thank all the members of the laboratory for comments on the manuscript and helpful suggestions during the course of these experiments. We also thank Debbie Townley for assistance with figure reproduction.

REFERENCES

1. Hasson, T., and Mooseker, M. S. (1995) *Curr. Opin. Cell Biol.* **7,** 587–594
2. Mermall, V., Post, P. L., and Mooseker, M. S. (1998) *Science* **279,** 527–533
3. Meyer, B. J., and Eck, M. J. (1995) *Curr. Biol.* **5,** 364–367
4. Novak, K. D., Peterson, M. D., Reedy, M. C., and Titus, M. A. (1995) *J. Cell Biol.* **131,** 1205–1221
5. Brown, S. S. (1997) *Curr. Opin. Cell Biol.* **9,** 44–48
6. Goodson, H. V., Anderson, B. L., Warrick, H. M., Pon, L. A., and Spudich, J. A. (1996) *J. Cell Biol.* **133,** 1277–1291
7. Geli, M. I., and Riezman, H. (1996) *Science* **272,** 533–535
8. Baines, I. C., Corigliano-Murphy, A., and Korn, E. D. (1995) *J. Cell Biol.* **130,** 591–603
9. McGoldrick, C. A., Gruver, C., and May, G. S. (1995) *J. Cell Biol.* **128,** 577–587
10. Yamashita, R. A., and May, G. S. (1998) *J. Biol. Chem.* **273,** 14644–14648
11. Durfee, T., Becherer, K., Chen, P.-L., Yeh, S.-H., Yang, Y., Kilburn A. E., Lee W.-H., and Elledge, S. J. (1993) *Genes Dev.* **7,** 555–569
12. Pontecorvo, G., Roper, J. A., Hemmons, C. M., MacDonald, K. D., and Bufton, A. W. J. (1953) *Adv. Genet.* **5,** 141–238
13. Ho, S. N., Hunt, H. D., Horton, R. M., Pullen, J. K., and Pease, L. R. (1989) *Gene* (*Amst.*) **77,** 51–59
14. Osmani, S. A., May, G. S., and Morris, N. R. (1987) *J. Cell Biol.* **104,** 1495–1504
15. Feinberg, A. P., and Vogelstein, B. (1983) *Anal. Biochem.* **132,** 6–13
16. May, G. S., Gambino, J., Weatherbee, J. A., and Morris, N. R. (1985) *J. Cell Biol.* **101,** 712–719
17. Laemmli, U. K. (1970) *Nature* **227,** 680–685
18. Waring, R. B., May, G. S., and Morris, N. R. (1989) *Gene* **79,** 119–130
19. Wolkow, D. T., Harris, S. D., and Hamer, J. E. (1996) *J. Cell Sci.* **109,** 2179–2188
20. Fiddy, C., and Trinci, A. P. J. (1976) *J. Gen. Microbiol.* **97,** 169–184
21. Feng, S., Chen, J. K., Hongtao, Y., Simon, J. A., and Schreiber, S. L. (1994) *Science* **266,** 1241–1247
22. Mooseker, M. S., and Cheney, R. E. (1995) *Annu. Rev. Cell Dev. Biol.* **11,** 633–675
23. Houdusse, A., Silver, M., and Cohen, C. (1996) *Structure* **4,** 1475–1490
24. Kalabokis, V. N., Vibert, P., York, M. L., and Szent-Gyorgyi, A. G. (1996) *J. Biol. Chem.* **271,** 26779–26782
25. Uyeda, T. Q., Abramson, P. D., and Spudich, J. A. (1996) *Proc. Natl. Acad. Sci. U. S. A.* **93,** 4459–6444
26. Mirabito, P. M., and Morris, N. R. (1993) *J. Cell Biol.* **120,** 959–968
27. Vida, T. A., and Emr, S. D. (1995) *J. Cell Biol.* **128,** 779–792